

Mapping soil attributes for site-specific management of a Montana field

John P. Wilson
Damian J. Spangrud

Department of Earth Sciences
Montana State University, Bozeman, MT 59717-0348

Melissa A. Landon
Jeffrey S. Jacobsen
Gerald A. Nielsen

Department of Plant, Soil, and Environmental Science
Montana State University, Bozeman, MT 59717-0312

ABSTRACT

Conventional soil maps represent the distribution of soil attributes across landscapes but with less precision than is needed to obtain the full economic and environmental benefits of site-specific crop management. This study quantifies the spatial variability of three agronomically significant soil attributes: 1) thickness of mollic epipedon, 2) organic matter content (OM), and 3) pH as related to soil survey map units, spectral data, and terrain attributes for a 20 ha field in Montana. Analysis of Order 1 (1:7920-scale) Soil Survey map units indicates substantial variation in all three soil attributes. There was some evidence that similar attribute values were clustered in the field (0.40-0.46 Moran's Coefficients). Two spectral band ratios explained 64% of the variation in OM across the field. GPS/GIS-derived wetness index, sediment transport index, elevation, and slope gradient explained 48% of OM variation. Wetness index, slope gradient, and plan curvature combined to explain 48% of the variation in mollic epipedon thickness. Elevation and wetness index explained just 13% of pH variation. Two spectral band ratios, specific catchment area, and wetness index combined to explain 70% of the variation in OM at 66 sampling sites. Four contour map representations of OM illustrate the sensitivity of the final maps to variations in input data and interpolation method.

1. INTRODUCTION

Site-specific crop management requires precise knowledge of soil attributes and soil-landscape processes.^{3,4,14,26} Detailed soil maps at scales of 1:6,000 or 1:8,000 and spatially-variable soil attribute data are needed to guide site-specific crop management in most landscapes.²¹ However, conventional soil survey maps are commonly published at 1:24,000 and these maps seldom delineate all of a field's variability.^{7,15} In addition, the range of soil attribute values reported for most mapping units is so great that these data cannot adequately represent soil attribute variation.²¹

Measurements of soil attributes are expensive, and numerous pedotransfer functions, image interpretations, and terrain attributes have recently been proposed as cost effective alternatives. Pedotransfer functions combine regression and other geostatistical techniques with soil texture, organic matter content, soil structure, and bulk density input data to predict agronomically significant soil attribute values that vary across and within mapped soil units.^{25,30,33,34} Remotely-sensed imagery may help with the estimation of soil attributes because particle size distribution, structure, surface roughness, moisture content, OM, and the abundance of carbonate minerals and iron oxides have all been shown to influence the reflectance captured by one or more spectral bands.^{1,8} Wilcox et al. used Landsat Thematic Mapper (TM) images to estimate surface OM in the Palouse Region of Eastern Washington and concluded that TM images could be used to predict OM values at non-sampled locations at a fraction of the cost of field sampling.³⁵ Other groups have used terrain attributes derived from digital elevation models (DEMs) for this purpose. Klingebiel et al. used slope, aspect, and elevation to increase the accuracy of mapped soil unit boundaries and thereby limit the within-unit variability, and several researchers have correlated soil properties with primary and secondary terrain attributes that have physical meaning in an effort to improve soil attribute prediction.^{2,12,21,22,27}

This paper aims to: (1) characterize the relationships between three soil attributes (thickness of mollic epipedon (dark topsoil), OM, and pH) and soil survey maps, imagery and terrain attributes, and (2) demonstrate the potential for using soil maps, images, or terrain data to describe soil attribute variation across a Montana farm field. Thickness of mollic epipedon, OM, and pH are important agricultural soil attributes. They affect soil physical properties, soil fertility, plant nutrient supply, and microbial activity and can be expected to vary across farm fields in Montana. Thickness of mollic epipedon is correlated with production of vegetation in the northern Great Plains.⁵ Thick dark colored epipedons are a "fossil record" of soil water availability, root growth, and humus formation. Larson examined the influence of soil series on small-grain yield in Montana and found that depth to calcium carbonate (CaCO₃) and OM were positively correlated with grain yield and that pH was inversely correlated with yield.¹³ These properties were also highly predictive of soil test phosphorus and available water-holding capacity (AWC). Wilson et al. evaluated the performance of the Productivity Index (PI) model in four Montana fields and found that an expanded model incorporating OM, depth to CaCO₃, and cropping history terms in addition to the AWC, bulk density, and pH terms in the original model explained 75% of the variability in grain yield.³⁶

2. METHODS AND DATA SOURCES

2.1 Study Area Description

The study area consists of a 20 ha farm field located at the base of the Bridger Mountains near the community of Springhill, Montana (T1N R6E, Section 18). It has a generally southerly aspect, moderate relief (43 m), and an average elevation of 1509 m (Figures 1B and 1C). A small intermittent stream runs through the field in a south-south-westerly direction (see bottom half of wire-mesh diagram). The soils are mostly: 1) fine-silty, mixed Typic Argiborolls, 2) fine, mixed Argic Cryoborolls, and 3) some coarse-silty, mixed Typic Ustochrepts that have been farmed with a grain-fallow rotation for about 50 years.

2.2 GPS Survey and Location of Sample Grid

Horizontal and elevation data were collected at 6,284 locations in September, 1991 with an Ashtech Sensor GPS receiver mounted on a pickup truck and an Ashtech P-12 GPS receiver operating in kinematic mode (Figure 1A). A permanent sampling grid was established ($n = 70$) and a 5.08 cm PVC neutron access tube was installed at each site to 200 cm below the soil surface using a truck-mounted Giddings hydraulic probe. The locations and elevations of the neutron access tubes were resurveyed in May, 1993 with an HP-48 data collector and Topcon GTS-303 total station.

2.3 Soil Sampling Procedures

Soil samples were collected and described in May, 1992. Field descriptions of the mollic, Bt, Bk, and 2C horizons including their color, textural class, and percent clay were obtained from the cores removed for neutron access tube installation. The cores were divided into 15 cm and 30 cm increments down to depths of 30 cm and 210 cm, respectively for laboratory analysis. Soil samples were air-dried, ground, and screened through a 2 mm sieve prior to analysis. Soil pH (1:2), EC (1:2 mmhos/cm), OM (%), Olsen P (mg/kg), K (mg/kg) were determined in the top 30 cm and NO₃-N (mg/kg) was determined for each depth increment to 210 cm. Only the thickness of the mollic epipedon, OM, and pH data are presented here.

2.4 Generation of Terrain Attributes

The GPS data were converted to a regular 10 m grid with ANUDEM¹¹ for subsequent analysis and display. This program takes irregular point or contour data and creates grid-based DEMs. ANUDEM automatically removes spurious pits within user-defined tolerances, calculates stream and ridge lines from points of locally maximum curvature on contour lines, and (most importantly) incorporates a drainage enforcement algorithm to maintain fidelity with a catchment's drainage network.^{11,24}

Primary terrain attributes were computed directly from the interpolated 10 m elevation grid (Figure 1C) with TAPES-G, a grid-based method of terrain analysis that calculates slope, aspect, specific catchment area, profile, plan and tangential curvature, and flow path length for each cell in a square-grid DEM.¹⁶ The maximum slope or gradient, β (in degrees), was computed with a finite-difference algorithm from the directional derivatives by:

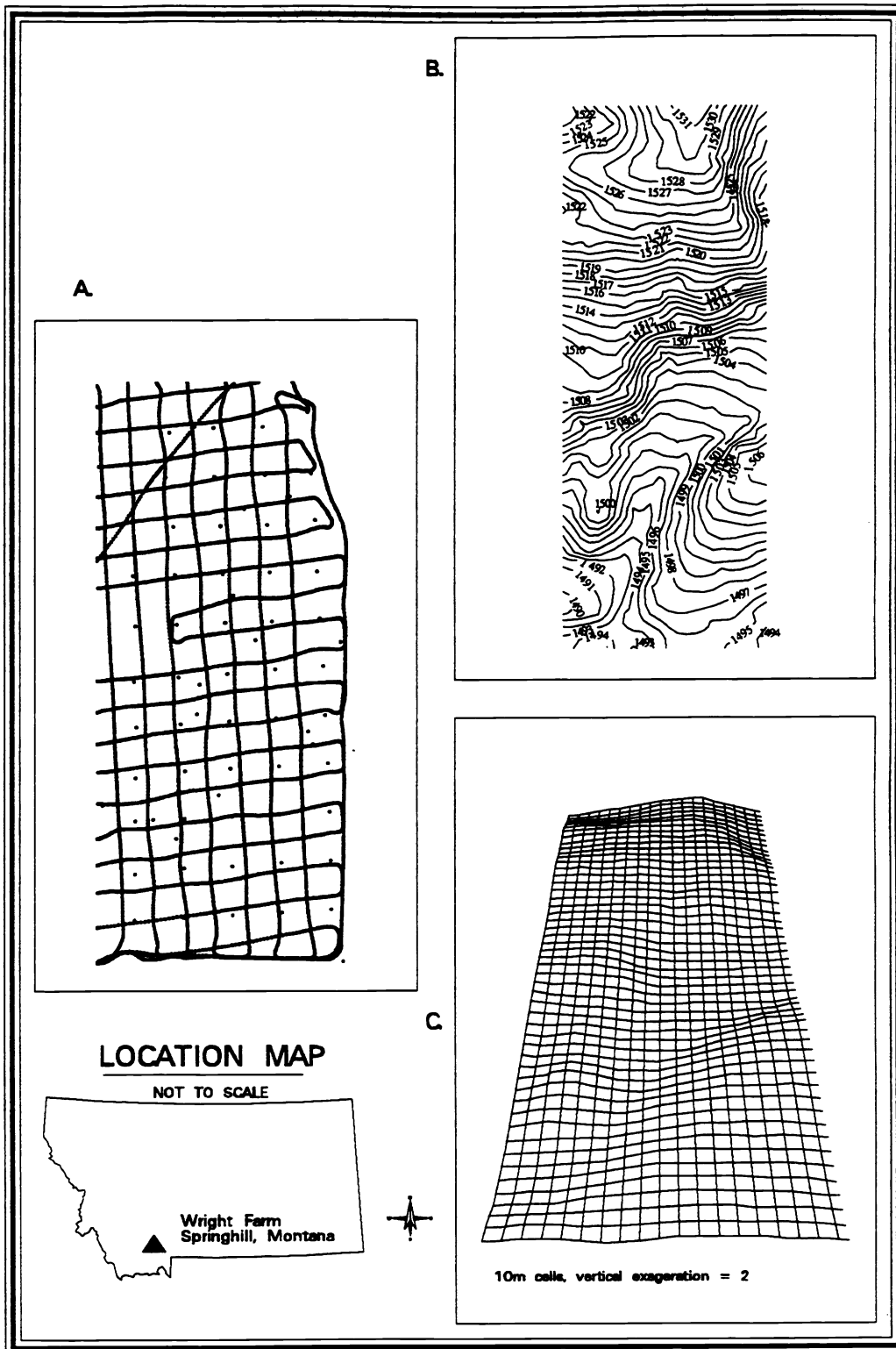


Figure 1. Full GPS data set (A), contour map (B), and three-dimensional wire mesh diagram (C) for study area.

$$\beta = \arctan [(f_x^2 + f_y^2)^{0.5}] \quad (1)$$

Specific catchment area (A_s) and flow path length were calculated with the FRho8 algorithm in upland areas above defined channels and the Rho8 algorithm below points of channel initiation. The Rho8 (random-eight node) algorithm is a stochastic version of the more common D8 algorithm (which allows drainage from a node to only one of eight nearest neighbors based on the direction of steepest descent) and the FRho8 algorithm permits drainage from a node to multiple nearest neighbors on a slope-weighted basis.²³ The Rho8 algorithm produces more realistic flow networks than the D8 algorithm and the FRho8 algorithm permits the modeling of flow dispersion in upland areas, which is important in areas with complex topography.^{16,24} A minimum drainage area of 2 ha (approximately 10% of the study area) was used to initiate channel flow. The proportion of flow or upslope contributing area assigned to multiple downslope nearest neighbors above these channels was determined on a slope-weighted basis using methods similar to those proposed by Freeman⁹ and Quinn et al.²⁹, so that the fraction of catchment area passed to neighbor i is given by:

$$F_i = \text{Max}(0, \text{Slope}_i^{1.1}) / \sum [\text{Max}(0, \text{Slope}_j^{1.1})] \quad (2)$$

where Slope is the slope from the current node to the nearest neighbor.

Four additional terrain attributes that may help in predicting the spatial distribution of soil attributes are the wetness index, w , the stream power index, Ω , a sediment transport capacity index, τ , and a landform curvature ratio, LCR. These compound indices are computed from two or more primary attributes and, in their simplest forms, can be expressed as:

$$w = \ln(A_s/\tan\beta) \quad \Omega = A_s \tan\beta \quad \tau = (A_s/22.13)^{0.6} (\sin\beta/0.0896)^{1.3} \quad \text{LCR} = \phi/\omega \quad (3)$$

where A_s is the specific catchment area (m^2m^{-1}), β is the slope angle (degrees), ϕ is the profile curvature or curvature in the direction of maximum slope (m), and ω is the plan curvature (curvature traverse to this slope) (m). The first three equations all assume that A_s is proportional to the discharge per unit width (q) and that steady-state conditions apply.^{17,20,22} The compound topographic wetness index has been used to: (1) characterize the spatial distribution of zones of surface saturation and soil water content in landscapes^{19,28}, (2) map forest soils³², and (3) delineate the spatial variability of soil properties in a toposequence in Colorado.^{21,22} The value of this index increases with increasing specific catchment area and decreasing slope gradient, resulting in moderate values on hilltops (flat areas with low specific catchment area), high values in valleys (high specific catchment area and low slope) where water concentrates, and low values on steep hillslopes (high slope) where water drains more freely.²³ The stream power index is directly proportional to stream power, which is the time rate of energy expenditure and so is a measure of the erosive power of overland flow.^{22,24} The sediment transport index characterizes erosion and deposition processes and, in particular, the effects of topography on soil loss.^{17,18} This index is applicable to three-dimensional landscapes and is analogous to the length-slope factor in the Revised Universal Soil Loss Equation.³¹ Profile curvature is a measure of the rate of change of the potential gradient and is therefore important for water flow and sediment transport, whereas plan curvature is a measure of the convergence or divergence and hence the concentration of water in the landscape.²² Dikau, for example, used slope, plan curvature, and profile curvature to delineate geomorphological relief units.⁶

The primary and secondary terrain attributes were used to construct grids in ARC/INFO (Environmental Systems Research Institute, Inc., Redlands, CA) and a series of point-in-grid overlays were performed to extract terrain attributes at 67 soil sampling sites. Three other soil sampling locations were lost when a new house was constructed along the western boundary of the field and a new rectangular study area was defined.

2.5 Collection and Analysis of Remotely-Sensed Spectral Data

Spectral data were captured with a small plane and the ADAR System 5000 (Positive Systems, Inc., Kalispell, MT) when the field was free of vegetation and stubble on 3 June, 1992. Blue (band 1; 450/80 nm center wavelength/bandwidth), red (band 2; 650/80 nm), red/near infrared (band 3; 700/40 nm), and near infrared (band 4; 850/80) bands were used. Differing amounts of translation and rotation were removed and a 3 by 3 pixel window (one pixel = 2.08 m) was averaged in an effort to reduce sample location error prior to analysis. Three bands were then ratioed to produce a 2-band image of 1/4 and 2/4 (which correspond to ADAR's blue/NIR and red/NIR bands, respectively) by:

$$\text{ratioed band DN} = \text{DN}_1 / (\text{DN}_2 + 0.5) \times 127 \quad (4)$$

where DN_1 and DN_2 are the first and second user-specified bands, respectively. This image was created to gauge the potential of the ADAR scanner for identifying OM. Frazier and Cheng⁸ have successfully used Landsat TM 1/4, 3/4, and 5/4 band ratios to map soil organic carbon in the Palouse region of Eastern Washington; however, there is little correspondence between Landsat TM spectral bands and those of the ADAR scanner. The bandwidths of the ADAR's blue and red filters are much wider than Landsat's blue and red bands, and Landsat's IR bands are beyond the ADAR's range of spectral response. The two ADAR band ratios used here mimic the Landsat TM 1/4 and 3/4 band ratios used by Frazier and Cheng.⁸

2.6 Preparation of Order 1 Soil Survey

An Order 1 soil survey map was prepared at a scale of 1:7920. Four major soil map units were reported in four slope classes using a 0.25 ha minimum delineation (equivalent to 100 10 m by 10 m cells) from uncorrected aerial photographs and field reconnaissance. Soil attributes were estimated from soil pits dug in the field and published series descriptions.

2.7 Statistical Analysis

The soils, terrain, image, and soil survey variables were exported to SAS to facilitate correlation and regression analysis. The Krustal-Wallis H statistic, which is a non-parametric alternative to the F ratio for classical analysis of variance, was used to compare the variation in soil attributes across Order 1 Soil Survey map units. The Moran Coefficient was used to measure the spatial structure or autocorrelation for the three soil attributes. The Moran statistic varies between -1 (negative spatial autocorrelation) and +1 (positive spatial autocorrelation) and measures the relationship among values of a single variable that is due to the geographic arrangement of areal units or points on a map.¹⁰ The most commonly used methods for computing spatial autocorrelation capture locational information in binary configuration tables. Sites are either adjacent to one another, or not. Thickness of mollic epipedon, OM, and pH site values were interpolated to a regular 50 m grid using ARC/INFO's Inverse Distance Weighting (IDW) function and values from the three nearest sampling sites. Moran Coefficients were computed with the method described by Griffith and Amrhein.¹⁰ Stepwise multiple regression was used to identify significant relationships between the soil survey, terrain, and image variables (independent variables) and the variability in thickness of mollic epipedon, OM, and pH (dependent variables). The F level for entry or deletion of an independent variable was set to 0.05. Statistical significance of the overall equation was determined by an F test. The t test was used to test the significance of each independent variable, and the models were evaluated for over- or under-specification using Mallows' Cp value. The map algebra tools in ARC/INFO's GRID module were used to prepare the final soil attribute maps.

3. RESULTS

Table 1 summarizes soil attribute values for the four map units and the entire field represented in the Order 1 Soil Survey map (Figure 2). The values computed for the Krustal-Wallis test statistic exceeded the critical value at the 0.05 level of significance (7.81 with 3 degrees of freedom) for all three soil properties indicating that: (1) the null hypothesis (that the means were equal) is rejected, (2) there is evidence that the mean soil properties for at least one of the soil map units is not equal to the others, and (3) only 5% of the time would one expect to obtain a Krustal-Wallis statistic that falls within the critical region (7.81, ∞) when in fact the four soil map unit means are equal. However, these soil map units may not help much with the interpolation of soil properties across the field because the minimum/maximum values and standard deviations reported for the individual soil map units indicate there is substantial variation in thickness of mollic epipedon, OM, and pH within map units.

Moran Coefficients of 0.40-0.46 indicate moderate clustering of similar values for the three soil attributes (Table 1). This result suggests that kriging may be more appropriate than a simple inverse distance weighted interpolation scheme for estimating thickness of mollic epipedon, OM, and pH values across the field. The three closest sampling sites and a 50 m grid were used to approximate the spacing between the initial soil sampling sites and minimize any inflation in Moran Coefficient scores caused by the conversion of the original site data to a regular 50 m grid with ARC/INFO's IDW command.

The multiple regression results treating OM as the dependent variable show that ADAR band ratios 3/4 and 1/4 explained 64%

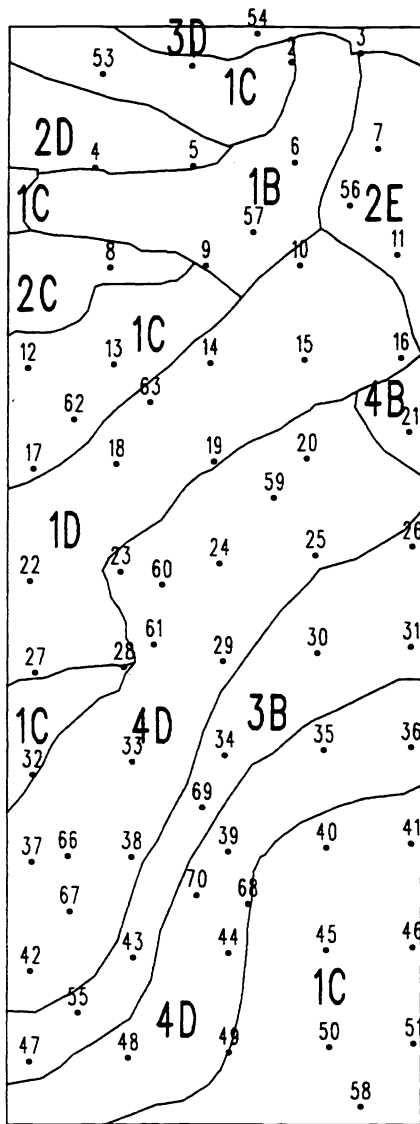
Table 1. Soil attribute values for four map units and the entire field represented in Order 1 Soil Survey map.

	No. of samples	Min.	Max.	Statistics		Median	Moran's I
				Mean	S.D.		
A. Thickness of mollic epipedon (cm)							
Alpha silt loam	29	15	80	36.4	18.0	34	-
Beta silt loam	7	19	66	43.1	19.4	49	-
Gamma loam	9	24	126	73.3	36.9	64	-
Omega-Beta-Sigma complex	22	10	118	44.4	29.0	41	-
Entire field	67	10	126	44.7	27.3	41	0.45
B. OM (%)							
Alpha silt loam	29	2.3	5.0	3.6	0.7	3.7	-
Beta silt loam	7	2.1	4.0	3.2	0.7	3.1	-
Gamma loam ^a	9	1.1	5.6	3.8	1.3	4.2	-
Omega-Beta-Sigma complex	22	1.7	5.6	3.3	1.0	3.4	-
Entire field	67	1.1	5.6	3.5	0.9	3.5	0.46
C. pH							
Alpha silt loam	29	5.6	6.6	6.0	0.2	6.0	-
Beta silt loam	7	5.7	7.1	6.2	0.4	6.2	-
Gamma loam	9	5.9	7.1	6.3	0.4	6.2	-
Omega-Beta-Sigma complex	22	5.8	8.3	6.7	0.9	6.4	-
Entire field	67	5.6	8.3	6.3	0.6	6.2	0.40

^a This soil map unit included one soil sampling site (#31 in Figure 2) with a very low organic matter content (1.1%). The next lowest OM computed for this unit was 2.6% (#54 in Figure 2). Site #31 is located near the outlet of a culvert that delivers runoff from upslope areas to the east of the field and was therefore omitted from the OM multiple regression analyses that produced the results reported in Table 2. The mean and median OM for this soil map unit without #31 were 4.1% and 4.3%, respectively.

of the variation in OM across the field (Table 2). The Palouse results using Landsat TM 3/4 and 5/4 band ratios obtained by Frazier and Cheng⁸ and Wilcox et al.³⁴ suggest an even higher R² might have been obtained in this study if the ADAR scanner had been able to replicate Landsat TM's IR bands. This shortcoming partially negates the timing (ADAR imagery is obtained with cameras mounted in small planes and can be collected on user-specified dates) and pixel resolution (the ADAR system can collect up to four bands of imagery at various pixel sizes starting at 1 m²) advantages of the ADAR system compared to Landsat TM data.

The multiple regression results treating OM, thickness of mollic epipedon, and pH as dependent variables and numerous terrain attributes as independent variables are also summarized in Table 2. Four terrain attributes combined to explain almost as much of the variation in OM (48%) as the two ADAR band ratios. This particular regression model included one interaction term (slope x aspect) because the DEM cells (slopes) were divided into north- and south-facing slopes. The exact meaning of the terms in this regression model is best interpreted by examining the response functions for north- and south-facing slopes separately. The response function for north-facing slopes can be written in equation form as:



Soil Series

- 1 Alpha silt loam
- 2 Beta silt loam
- 3 Gamma loam
- 4 Omega-Beta-Sigma complex

Slope Classes

- B 2 to 4 percent
- C 4 to 8 percent
- D 8 to 15 percent
- E 15 to 25 percent

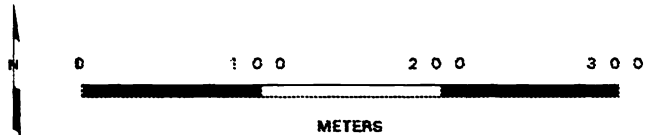


Figure 2. Order 1 Soil Survey map

$$E(Y) = 24.1831 + 0.3883 \text{ WI} - 0.0455 \text{ STI} - 0.0153 \text{ ELEV} + 0.328 \text{ SLOPE} \quad (5)$$

where Y is predicted OM, WI is the wetness index, STI is the sediment transport index, ELEV is elevation in meters above sea level, and SLOPE is slope gradient in degrees. This equation shows how OM varies positively with wetness index and slope, and inversely with elevation and sediment transport index on north-facing slopes. The SLOPE term disappears from the response function for south-facing slopes (because the ASPECT indicator variable was set to 0 in these cells) as follows:

$$E(Y) = 24.1831 + 0.3883 \text{ WI} - 0.0455 \text{ STI} - 0.0153 \text{ ELEV} \quad (6)$$

This response function indicates how predicted OM varies positively with wetness index and inversely with elevation and sediment transport index on south-facing slopes. These results are similar to those of Moore et al. who explained 48% of the variation in OM in a 5.4 toposquence (field) in Colorado using wetness index, stream power index, and aspect as independent variables.²²

Table 2. Multiple regression results

Step	Variable	Parameter estimate	Partial R ²	Model R ²	Prob>F
<i>Dependent variable:</i> OM (%)					
	INTERCEPT	8.5791			
1	BAND2/BAND4	-0.0685	0.550	0.550	0.0001
2	BAND1/BAND4	0.0533	0.093	0.643	0.0001
<i>Dependent variable:</i> OM (%)					
	INTERCEPT	24.1831			
1	WETNESS INDEX	0.3883	0.332	0.322	0.0001
2	SED. TSPT INDEX	-0.0455	0.068	0.400	0.0099
3	ELEVATION	-0.0153	0.050	0.449	0.0210
4	SLOPE2 ^a	0.0328	0.035	0.484	0.0469
<i>Dependent variable:</i> THICKNESS OF MOLLIC EPIPEDON (cm)					
	INTERCEPT	-86.1411			
1	WETNESS INDEX	15.9640	0.389	0.389	0.0001
2	SLOPE	2.0395	0.045	0.434	0.0274
3	PLAN CURVATURE	-1.0132	0.041	0.475	0.0300
<i>Dependent variable:</i> pH					
	INTERCEPT	33.6485			
1	ELEVATION	-0.0177	0.069	0.069	0.0318
2	WETNESS INDEX	-0.0903	0.059	0.128	0.0407
<i>Dependent variable:</i> OM (%)					
	INTERCEPT	7.0003			
1	BAND2/BAND4	-0.5640	0.550	0.550	0.0001
2	BAND1/BAND4	0.0408	0.093	0.643	0.0001
3	SPECIFIC CATCH. AREA	-0.0002	0.032	0.675	0.0128
4	WETNESS INDEX	0.2347	0.029	0.704	0.0222

^a One interaction term (SLOPE2 = SLOPE x ASPECT) appears in the second OM regression equation. This term applies to north-facing slopes because the indicator variable (ASPECT) was set to 0 on south-facing slopes and to 1 on north-facing slopes.

Three terrain terms (wetness index, slope gradient, and plan curvature) explained 48% of the variability in thickness of mollic epipedon and two terrain terms (elevation and wetness index) combined to explain only 13% of the variability in pH (Table 2). The thickness of mollic epipedon results matched those of Moore et al.²² who predicted 50% of the variation in A (mollic) horizon depth using slope and wetness index in Colorado and Bell et al.² who explained 51% of the variation in A horizon depth using wetness and drainage proximity terms for a 20 ha study site in west-central Minnesota. However, Moore et al. were also able to predict 41% of the variation in pH using slope gradient and plan curvature for their Colorado toposequence.²²

The final regression model reproduced in Table 2 used the image and terrain variables to predict OM across the field. The two band ratios and two terrain variables (specific catchment area and wetness index) combined to explain 70% of the variation in OM at the 66 soil sampling sites (one site was dropped for the reasons noted in Table 1). This model shows that: (1) the image attributes were better than the terrain variables in explaining the variability in OM, and (2) the terrain variables were able to explain approximately 15% of the residual variability left unexplained by the two band ratios. This may not be a fair comparison because of the different cell resolutions (sizes) that were used for the ADAR imagery (6.24 m by 6.24 m cells) and terrain analysis (10 m by 10 m cells). A higher resolution DEM could have been generated here and may have produced slightly better correlations. However, Moore et al. have argued that: (1) it is unrealistic to expect such soil-landscape (terrain analysis) methods to explain more than 70% of the variability in soil properties because of variations in soil-related processes (such as hydrology and soil erosion and deposition) that occur at larger scales (i.e., over shorter distances) than the resolution of the DEM that is used, and (2) the optimum scales for studying and characterizing landscape processes affecting the development of the soil catena are unknown and represent a major research need.²¹ No attempt was made to generate a higher resolution DEM in this study given this state of affairs and the fact that the GPS survey used to generate the DEM did not include the entire catchment drained by the ephemeral channel that flows in a south-south-westerly direction through the southern half of the field (Figure 1C).

The final maps show OM delineated in 1% intervals across the field. The first map (Figure 3A) was generated with ARC/INFO's IDW function and OM values at the three nearest soil sampling sites. This map shows less variation than the others because OM values at 66 sampling sites spaced roughly 50 m apart were used to estimate OM in 65 50 m by 50 m cells. The second map (Figure 3B) was produced with the regression equation incorporating the two ADAR band ratios and shows the most detail because 2.08 m pixels (cells) were used. The final two maps (Figures 3C and 3D) were produced with the regression equations incorporating terrain and image/terrain attributes as independent variables and 10 m cells (see Table 2 for regression equations). As expected, the low and high OM values in Figure 3C follow ridge and channel features; however, this pattern was modified and OM estimates increased when both image and terrain attributes were used (Figure 3D) since this model combined data layers with different cell resolutions. Overall, the four maps show how different data sources and analytical methods may lead to different estimates of economically- and environmentally-significant soil properties such as OM.

This spatially varying soil attribute information is needed to divide farm fields into management units. The management units can be used with automated navigation (guidance) systems and variable rate spreaders to apply only those quantities of seed, fertilizers, and pesticides that match the land resource potential and/or the farmer's yield goals. The difficulty, expense, and uncertainty currently involved in delineating management units will limit the adoption of these technological aids and minimize the economic and environmental advantages that might follow from their adoption in the immediate future. More work is needed to identify significant soil properties and to compare and contrast alternative data sources and methods for estimating them and dividing farm fields into management units.

5. ACKNOWLEDGMENTS

Financial support for this work was provided by USDA-CSRS Water Quality Special Grant #91-34214-6057. Contribution no. J-3020 of the Montana Agricultural Experiment Station. The GPS survey was prepared and the initial image processing was accomplished with the assistance of David Tyler in the Department of Surveying Engineering at the University of Maine. Brian Autio and his students in the Department of Civil Engineering at Montana State University resurveyed the soil sampling sites. Tony Rolfes from the local Soil Conservation Service office prepared the Order 1 Soil Survey, and one of the senior author's undergraduate students, Mike Miller, wrote the program that was used to compute the Moran Coefficients.

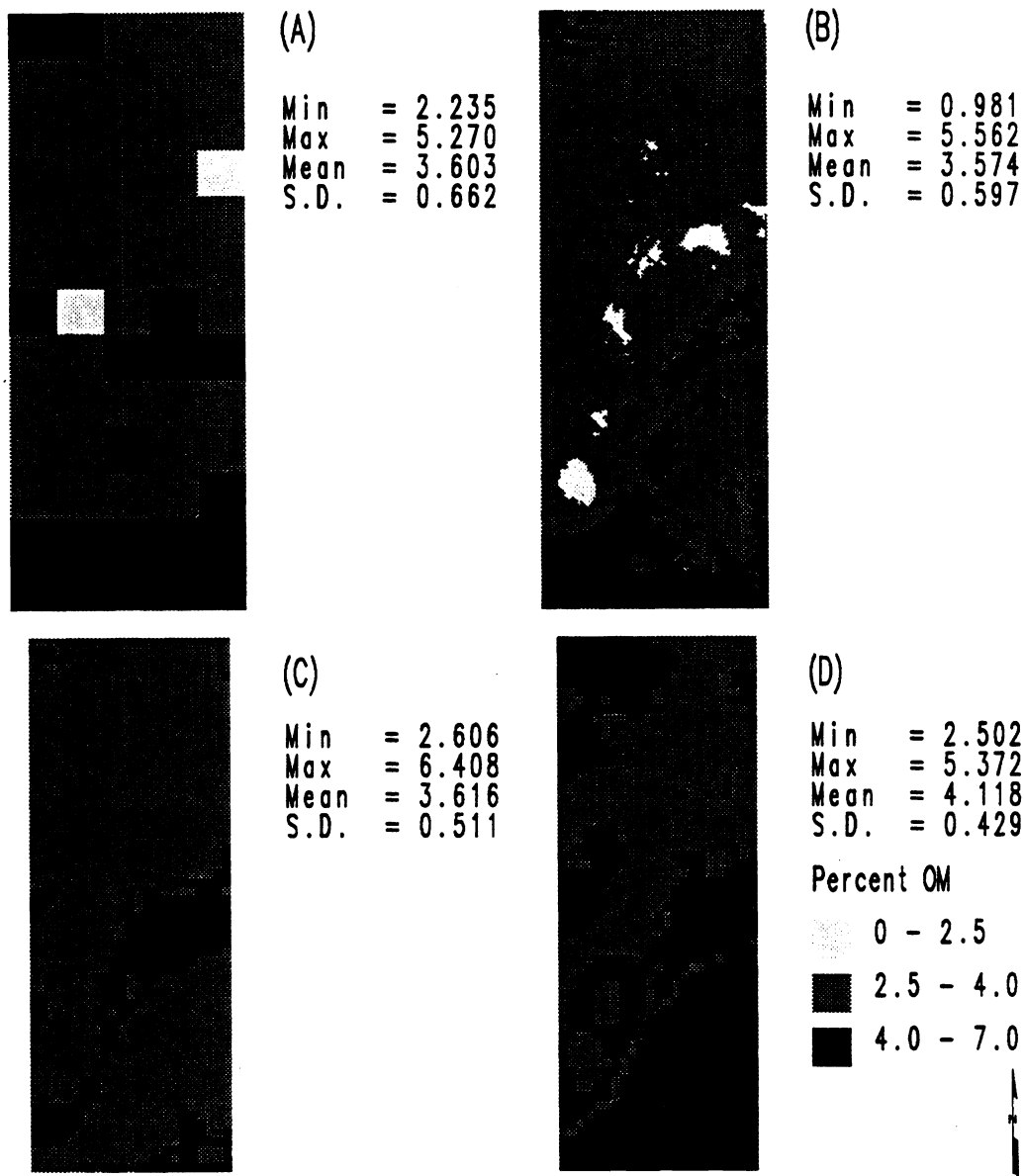


Figure 3. Organic matter content (OM) contour maps produced by linear interpolation of measured data (A), a regression function incorporating ADAR band ratios (B), a regression function incorporating selected terrain attributes (C), and a regression function combining the ADAR band ratios and selected terrain attributes (D).

6. REFERENCES

1. M.F. Baumgardner, L.F. Silva, L.L. Biehl and E.R. Stoner, "Reflectance properties of soils", *Adv. Agron.*, Vol. 38, pp. 1-44, 1985.
2. J.C. Bell, J.A. Thompson, C.A. Butler and K. McSweeney, "Modeling soil genesis from a landscape perspective", pp. 179-195 in Transactions of the 15th World Congress on Soil Science, Acapulco, Mexico, July 1994, Int. Soc. Soil Sci., Madison, 1994.

3. J. Bouma and P.A. Finke, "Origin and nature of soil resource variability," pp. 3-13 in P.C. Robert, R.H. Rust and W.E. Larson (eds), Soil Specific Crop Management: A Workshop on Research and Development Issues, Am. Soc. Agron., Madison, 1993.
4. P.A. Burrough, "Soil variability: A late 20th century view," *Soils and Fertilizers*, Vol. 56, pp. 529-562, 1993.
5. M.E. Cannon and G.A. Nielsen, "Estimating production of range vegetation from easily measured soil characteristics," *Soil Sci. Soc. Am. J.*, Vol. 48, pp. 1393-1397, 1984.
6. R. Dikau, "The application of a digital relief model to landform analysis in geomorphology", pp. 51-77 in J. Raper (ed.), Three Dimensional Applications in Geographic Information Systems, Taylor and Francis, New York, 1989.
7. P.F. Fisher, "Modeling soil map inclusions by Monte Carlo simulation," *Int. J. Geogr. Info. Systems*, Vol. 5(2), pp. 193-208, 1991.
8. B.E. Frazier and Y. Cheng, "Remote sensing of soils in the eastern Palouse region with Landsat Thematic Mapper," *Remote Sens. Environ.*, Vol. 28, pp. 317-325, 1989.
9. G.T. Freeman, "Calculating catchment area with divergent flow based on a regular grid," *Comp. and Geosci.*, Vol. 17, pp. 413-422, 1991.
10. D.A. Griffith and C.G. Amrhein, *Statistical Analysis for Geographers*, Prentice-Hall, Englewood Cliffs, 1991.
11. M.F. Hutchinson, "A new procedure for gridding elevation and stream line data with automatic removal of spurious pits," *J. Hydrol.*, Vol. 106, pp. 211-232, 1989.
12. A.A. Klingebiel, E.H. Horvath, D.G. Moore and W.U. Reybold, "Use of slope, aspect, and elevation maps derived from digital elevation model data in making soil surveys," pp. 77-90 in W.U. Reybold and G.W. Peterson (eds), Soil Survey Techniques, Soil Sci. Soc. Am. Spec. Publ. No. 20, Madison, 1987.
13. M.H. Larson, "The influence of soil series on cereal grain yield", Unpubl. M.S. Thesis, Montana State Univ., Bozeman, 1986.
14. W.E. Larson and P.C. Robert, "Farming by soil," pp. 103-112 in R. Lal and F.J. Pierce (eds), Soil Management for Sustainability, Soil and Water Conserv. Soc., Ankeny, 1991.
15. M.J. Mausbach, D.J. Lyttle and L.D. Spivey, "Application of soil survey information to site-specific farming", pp. 57-68 in P.C. Robert, R.H. Rust and W.E. Larson (eds), Soil Specific Crop Management: A Workshop on Research and Development Issues, Am. Soc. Agron., Madison, 1993.
16. I.D. Moore, "Terrain Analysis Programs for the Environmental Sciences: TAPES," *Agric. Systems Info. Tech.*, Vol. 4(2), pp. 37-39, 1992.
17. I.D. Moore and J.P. Wilson, "Length-slope factors for the Revised Universal Soil Loss Equation: Simplified method of estimation", *J. Soil and Water Conserv.*, Vol. 47(5), pp. 423-428, 1992.
18. I.D. Moore and J.P. Wilson, "Reply to Comment on Length-slope factors for the Revised Universal Soil Loss Equation: Simplified method of estimation", *J. Soil and Water Conserv.*, Vol. 49(2), pp. 174-180, 1994.
19. I.D. Moore, G.J. Burch and D.H. McKenzie, "Topographic effects on the distribution of surface water and the location of ephemeral gullies," *Trans. Am. Soc. Agric. Engr.*, Vol. 31, pp. 1383-1395, 1988.

20. I.D. Moore, R.B. Grayson and A.R. Ladson, "Digital terrain modeling: A review of hydrological, geomorphological, and biological applications," *Hydrol. Proc.*, Vol. 5(1), pp. 3-30, 1991.
21. I.D. Moore, P.E. Gessler, G.A. Nielsen, and G.A. Peterson, "Terrain analysis for soil specific crop management", pp. 27-56 in P.C. Robert, R.H. Rust and W.E. Larson (eds), Soil Specific Crop Management, Soil Sci. Soc. Am., Madison, 1993.
22. I.D. Moore, P.E. Gessler, G.A. Nielsen and G.A. Peterson, "Soil attribute prediction using terrain analysis," *Soil Sci. Soc. Am. J.*, Vol. 57, pp. 443-452, 1993.
23. I.D. Moore, A. Lewis and J.C. Gallant, "Terrain attributes: Estimation method and scale effects," pp. 30-38 in A.K. Jakeman, M.B. Beck and M.J. McAleer (eds), Modelling Change in Environmental Systems, John Wiley & Sons, Chichester, 1993.
24. I.D. Moore, A.K. Turner, J.P. Wilson, S.K. Jenson and L.E. Band, "GIS and land surface-subsurface process modeling," pp. 196-230 in M.F. Goodchild, B.O. Parks and L.T. Steyaert (eds), Environmental Modeling with GIS, Oxford Univ. Press., New York, 1993.
25. D.J. Mulla, "Using geostatistics and GIS to manage spatial patterns in soil fertility," pp. 336-345 in G. Kranzler (ed.), Automated Agriculture in the Twenty-first Century, Am. Soc. Agric. Engr., St. Joseph, 1991.
26. D.J. Mulla, "Mapping and managing spatial patterns in soil fertility and crop yield," pp. 15-26 in P.C. Robert, R.H. Rust and W.E. Larson (eds), Soil Specific Crop Management: A Workshop on Research and Development Issues, Am. Soc. Agron., Madison, 1993.
27. I.O.A. Odeh, D.J. Chittleborough and A.B. McBratney, "Elucidation of soil-landform interrelationships by canonical ordination analysis," *Geoderma*, Vol. 49(1), pp. 1-32, 1991.
28. E.M. O'Loughlin, "Prediction of surface saturation zones in natural catchments by topographic analysis," *Water Resour. Res.*, Vol. 22(5), pp. 794-804, 1986.
29. P. Quinn, K. Bevin, P. Chevallier and O. Planchon, "The prediction of hillslope flow paths for distributed hydrological modeling using digital terrain models," *Hydrol. Proc.*, Vol. 5(1), pp. 59-79, 1991.
30. W.J. Rawls, D.J. Brakensiek and K.E. Saxton, "Estimating soil water properties," *Trans. Am. Soc. Agric. Engr.*, Vol. 25, pp. 1316-1320, 1328, 1982.
31. K.G. Renard, G.R. Foster, G.A. Wiegand and J.A. Porter, "RUSLE: Revised Universal Soil Loss Equation," *J. Soil and Water Conserv.*, Vol. 46(1), pp. 30-33, 1991.
32. A.K. Skidmore, P.J. Ryan, W. Dawes, D. Short and E. O'Loughlin, "Use of an expert system to map forest soils from a geographical information system," *Int. J. Geogr. Info. Systems*, Vol. 5(4), pp. 431-445, 1991.
33. R.J. Wagenet, J. Bouma and R.B. Grossman, "Minimum data sets for use of soil survey information in soil interpretive models," pp. 161-182 in M.J. Mausbach and L.P. Wilding (eds.), Spatial Variabilities of Soils and Landforms, Soil Sci. Soc. Am. Spec. Public. No. 28, Madison, 1991.
34. R. Webster, "Canonical correlation in pedology: How useful?," *J. Soil Sci.*, Vol. 28, pp. 196-221, 1977.
35. C.H. Wilcox, B.E. Frazier and S.T. Ball, "Relationships between soil organic carbon and Landsat TM data in eastern Washington," *Photogram. Engr. and Remote Sens.*, Vol. 60(6), pp. 777-781, 1994.
36. J.P. Wilson, S.P. Sandor and G.A. Nielsen, "Productivity Index Model modified to estimate variability of Montana small grain yields", *Soil Sci. Soc. Am. J.*, Vol. 55(1), pp. 228-234, 1991.